available at www.sciencedirect.com
journal homepage: www.europeanurology.com

European Association of Urology

Platinum Priority Brief Correspondence

Editorial by Douglas G. Ward, Roland Arnold and Richard T. Bryan on pp. 538–539 of this issue.

Identification of Differential Tumor Subtypes of T1 Bladder Cancer

A. Gordon Robertson [a], Clarice S. Groeneveld [b,c], Brian Jordan [d], Xiquo Lin [e], Kimberly A. McLaughlin [f], Arighno Das [f], Leigh Ann Fall [f], Damiano Fantini [f], Timothy J. Taxter [h], Lauren S. Mogil [i], Sia Viborg Lindskrog [j], Lars Dyrskjøt [j], David J. McConkey [k], Robert S. Svatek [l,m], Aurélien de Reyniès [b], Mauro A.A. Castro [n], Joshua J. Meeks [f,g,]*

[a] *Dxige Research Inc., Courtenay, BC, Canada;* [b] *Cartes d'Identité des Tumeurs Program, Ligue Nationale Contre le Cancer, Paris, France;* [c] *Oncologie Moleculaire, Institut Curie, Equipe Labellisée Ligue Contre le Cancer, Paris, France;* [d] *Department of Urology, University of Washington, Seattle, WA, USA;* [e] *Department of Pathology, Northwestern University, Feinberg School of Medicine, Chicago, IL, USA;* [f] *Departments of Urology, Biochemistry and Molecular Genetics, Feinberg School of Medicine, Northwestern University, Chicago, IL, USA;* [g] *Jesse Brown VA Medical Center, Chicago, IL, USA;* [h] *Tempus Labs, Inc., Chicago, IL, USA;* [i] *Center for Translational Data Science, University of Chicago, Chicago, IL, USA;* [j] *Department of Molecular Medicine, Aarhus University Hospital, Aarhus, Denmark;* [k] *Johns Hopkins Greenberg Bladder Cancer Institute, Brady Urological Institute, Johns Hopkins University, Baltimore, MD, USA;* [l] *Experimental Developmental Therapeutics Program, UT Health MD Anderson, San Antonio, TX, USA;* [m] *Department of Urology, UT Health San Antonio, San Antonio, TX, USA;* [n] *Bioinformatics and Systems Biology Laboratory, Federal University of Paraná, Curitiba, Brazil*

Article info

Article history:
Accepted June 22, 2020

Associate Editor:
James Catto

Statistical Editor:
Emily Zambor

Keywords:
Non–muscle-invasive bladder cancer
Bacillus Calmette-Guérin
Carcinoma in situ
Immune signatures
Tumor subtype
Luminal

Abstract

Stage T1 bladder cancers have the highest progression and recurrence rates of all non–muscle-invasive bladder cancers (NMIBCs). Most T1 cancers are treated with bacillus Calmette-Guérin (BCG), but many will progress or recur, and some T1 patients will die from bladder cancer. Particularly aggressive tumors could be treated with early cystectomy. To better understand the molecular heterogeneity of T1 cancers, we performed transcriptome profiling and unsupervised clustering, and identified five consensus subtypes of T1 tumors treated with repeat transurethral resection (reTUR) and induction and maintenance BCG. The T1-LumGU subtype was associated with carcinoma in situ (CIS; six/13, 46% of all CIS), had high E2F1 and EZH2 expression, and was enriched in E2F target and G2M checkpoint hallmarks. The T1-Inflam subtype was inflamed and infiltrated with immune cells. While most T1 tumors were classified as luminal papillary, the T1-TLum subtype had the highest median luminal papillary score and FGFR3 expression, no recurrence events, and the fewest copy number gains. T1-Myc and T1-Early subtypes had the most recurrences (14/30 within 24 mo), the highest median MYC expression, and, when combined, had significantly worse recurrence-free survival than the other three subtypes. T1-Early had five (38%) recurrences within the first 6 mo of BCG, and repressed IFN-α and IFN-γ hallmarks and inflammation. We developed a single-patient T1 classifier and validated our subtype biology in a second cohort of T1 tumors. Future research will be necessary to validate the proposed T1 subtypes and to determine if therapies can be individualized for each subtype.

Patient summary: We identified and characterized expression subtypes of high-grade stage T1 bladder cancer that are biologically heterogeneous and have variable responses to bacillus Calmette-Guérin treatment. We validated the subtypes and describe a single-patient classifier.

* Corresponding author. Department of Urology, Feinberg School of Medicine, Northwestern University, 676 N St Clair Suite 2300 Chicago, IL 60611, USA. Tel. +1 312-694-9001 Fax: +1 312-694-9000.
E-mail address: joshua.meeks@northwestern.edu (J.J. Meeks).

https://doi.org/10.1016/j.eururo.2020.06.048
0302-2838/Published by Elsevier B.V. on behalf of European Association of Urology.

T1 tumors are potentially the most aggressive subtype of non–muscle-invasive bladder cancer (NMIBC), with 40% recurrence and 15% progression at 5 yr [1]. While most T1 cancers are treated with bacillus Calmette-Guérin (BCG), recurrence or progression is treated with radical cystectomy, and delayed intervention is associated with lower survival [1]. Biomarkers that could predict response to BCG in T1 cancers could help both patients and clinicians in making treatment-related decisions; however, few to no tumor-specific prognostic features have been identified. We previously reported that T1 and MIBC cancers had similar mutations, but that mutations were unable to predict response to BCG [2]. The primary objective of our study was to investigate the molecular heterogeneity of T1 cancers via RNA sequencing of 73 primary T1 tumors (Supplementary Table 1A) with a primary endpoint of recurrence after BCG. To minimize sources of bias, all tumors were treated at the same institution, 84% had repeat transurethral resection, and all received induction and maintenance BCG (64%) if they did not recur. The recurrence rate was 32% (23/73) at 24 mo and 25% (18/73) at 1 yr, with progression in 8% (six/73) at 24 mo (Supplementary Table 1A, Supplementary Fig. 1). We focused our analysis on tumor expression subtypes identified via unsupervised consensus clustering. After assessing three-, four-, and five-cluster solutions (Supplementary Fig. 2), we characterized a five-cluster solution whose subtypes had distinct clinical outcomes and biological characteristics (Fig. 1). We combined gene expression, gene-set enrichment, and regulon analyses to describe the distinct biology for each subtype (Supplementary methods) [3].

The T1-luminal genomically unstable (T1-LumGU) subtype had the highest frequency of pathologic carcinoma in situ (CIS; six/16 [38%] of T1-LumGU vs 13/73 [18%] of all samples; Supplementary Table 2) with moderate enrichment in CIS up and down gene sets and a recurrence rate of 25% (four/16) at 24 mo (Fig. 1D, Supplementary Fig. 3A,B, Supplementary methods). Analysis of T1-LumGU using other classifiers identified 14/16 samples (88%) as Lund GU and nine/16 (56%) as consensusMIBC LumU [4]. T1-LumGU tumors had the largest median number of somatic copy number (CN) gains (Fig. 1G; $p = 0.016$, Kruskal test). While inflammation genes were weakly repressed in T1-LumGU tumors, Molecular Signatures Database (MSigDB) C3 E2F1 motifs were enriched (Supplementary Fig. 4), as were hallmark gene sets for E2F targets and G2M checkpoint (area under the curve [AUC] 0.77 and 0.69, Supplementary Fig. 5).

A set of 170 inflammation-related genes was highly expressed in T1-Inflamed (T1-Inflam) tumors (Fig. 1A,D and Supplementary Fig. 3C; AUC 0.91, CERNO test [5]). T1-Inflam tumors had the highest levels of many immune cell types, including cytotoxic lymphocytes and T cells, as well as the highest immune and stromal scores and the lowest tumor purity (Fig. 1F, Supplementary Fig. 6B). Multiple inflammatory hallmarks were enriched, and Myc and E2F target hallmarks were repressed (Fig. 1C, Supplementary Fig. 5). While T1-Inflam tumors were mostly LumP (11/14, 79%), CIS rates were low (three/14, 21%) and there were four/14 (29%) recurrences by 24 mo. Hallmarks and immune signatures were consistent with increased expression of immune regulators NFATC2 and STAT4 (Supplementary Fig. 4B), and we hypothesize that T1-Inflam tumors represent an immune-active and inflamed T1 subtype.

Collectively, subtypes T1-Myc and T1-Early (S5) had the most recurrences, with over half of tumors recurring after BCG treatment (14/24, 58% of patients at 24 mo over both subtypes; Fig. 1B). T1-Myc had the most recurrences by 24 mo (12/17, 71%). T1-Myc tumors were mostly (14/17, 82%) LumP, and all were UROMOL class 2a. They had high MYC expression levels and enriched Myc target hallmarks (AUC 0.71; Fig. 1C,H and Supplementary Fig. 5). Inflammatory gene signatures were minimally repressed (AUC 0.66, Supplementary Fig. 3C). Pathological CIS was present in two/17 (12%), but CIS gene sets were not enriched (Supplementary Fig. 3A).

Subtype T1-True Luminals (T1-TLum) was the most luminal and urothelial-differentiated subtype. Overall, T1-TLum tumors had the fewest 24-mo recurrences (two/13, 15%). The T1-TLum group had the highest median consensusMIBC LumP classifier score (Fig. 1E) and contained four/13 (31%) UROMOL class 1 tumors. T1-TLum tumors had the fewest somatic CN gains [6] (Fig. 1G) and had strongly repressed CIS (ie, enriched in CIS down with repressed CIS up genes; Supplementary Fig. 3A). Inflammatory and proliferative hallmarks were repressed (Fig. 1C and Supplementary Fig. 5), immune cell markers were low according to multiple deconvolution methods (Supplementary Fig. 6), and luminal differentiation genes FGFR3 and RXRA were highly expressed (Fig. 1H).

Subtype T1-Early had five/13 (38%) recurrences within 6 mo of induction BCG, with no further recurrences by 24 mo. This subtype had the highest median MYC expression and enriched Myc target hallmarks (AUC 0.80; Fig. 1C,H and Supplementary Fig. 5). These tumors had no reported CIS, and had repressed CIS gene signatures (Supplementary Fig. 3). While both T1-Myc and T1-Early had elevated MYC expression, T1-Early differed from T1-Myc in having repressed immune response hallmarks for IFN-α (AUC 0.81) and IFN-γ (AUC 0.75) (Supplementary Fig. 5). Thus, T1-Early appeared to be a MYC-driven subtype with an immune-suppressive microenvironment that was depleted in immune cells, suggesting its tumor microenvironment may represent an immune desert. Grouping the two Myc-driven subtypes together, T1-Early and T1-Myc had significantly worse recurrence-free survival than the other three subtypes grouped ($p = 0.025$, Fig. 1I).

We used regulon analysis to further characterize the molecular differences and similarities among the subtypes. This identified two major patterns of regulon activity that suggested that the five expression subtypes could be grouped into two regulon classes: T1-LumGU + T1-Myc and T1-TLum + T1-Early (Supplementary Fig. 7A). Subtypes T1-LumGU + T1-Myc had activated regulons for transcription factors E2F1 and FOXM1, and enriched hallmarks for E2F targets, G2M checkpoint, and interferon response pathways. By contrast, subtypes T1-TLum + T1-Early (and to some degree T1-Inflam) were characterized by activated

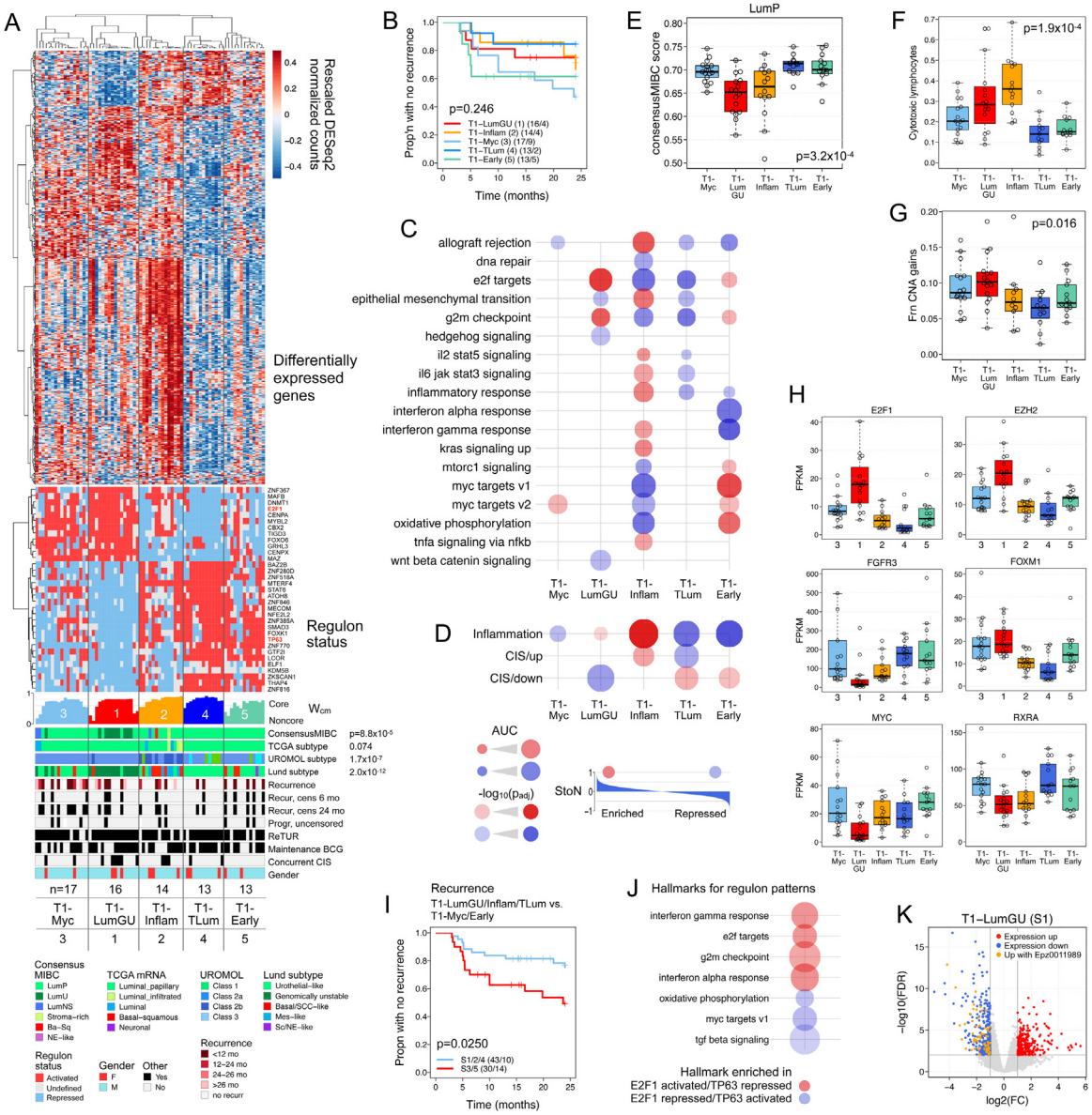

Fig. 1 – Characterization of five gene expression subtypes for T1 tumors based on transcriptome profiles and clinical variables. (A) Top: heatmap of subtype-specific differentially expressed genes (DEGs) for five unsupervised consensus expression clusters identified using the most-variant 2945 (ie, 15%) protein-coding genes (Supplementary methods). Below the DEG heatmap is a heatmap showing activity status profiles for 33 regulons, with red, blue, and grey indicating activated, repressed, and undefined regulon activity status, respectively. Below this are covariate tracks for expression-based classifier subtyping of each T1 tumor, with consensusMIBC, TCGA, UROMOL, and Lund subtypes shown. Below these are clinical and pathologic covariates. (B) Kaplan-Meier plot of recurrence, censored at 24 mo, with a log-rank *p* value, demonstrating increased recurrence of subtypes T1-Myc (S3, 24 mo) and T1-Early (S5, 6 mo). (C) Selected Molecular Signatures Database hallmark gene sets enriched in genes overexpressed (red disks) or underexpressed (blue) in a subtype. Gene set enrichment analysis results are from CERNO tests [5]; disk diameter is proportional to area under the curve (ie, effect size) and color opacity is proportional to $-\log10(p_{Adj})$. (D) CERNO tests of 170 inflammation-related genes and CIS up/down genes, with dot size and color as described in (C). (E) Distribution of LumP consensusMIBC classifier scores across T1 subtypes; T1-TLum had the highest median LumP score. (F) Cytotoxic lymphocytes predicted by MCPcounter (Supplementary Fig. 6); T1-Inflam had the most immune cells. (G) Somatic copy number (CN) gains, expressed as a fraction of the total genome length with CN calls; T1-LumGU had the most CNAs and T1-TLum the fewest. (H) Per-subtype expression distributions of select genes. A comparison of FPKM and TPM expression distributions is shown in Supplementary Figure 4B. (I) A Kaplan-Meier curve identified significantly worse recurrence at 24 mo for the two subtypes with the highest recurrence (T1-Myc and T1-Early) compared to the three other subtypes (T1-LumGU, T1-Inflam, T1-TLum). (J) The regulon-based group consisting of subtypes T1-LumGU + T1-Myc was enriched in hallmarks for E2F targets, G2M checkpoint, and interferon response pathways; by contrast, the group consisting of subtypes T1-TLum + T1-Early (and to some degree T1-Inflam) was characterized by activated SMAD3 and TP63 regulons, and enriched in hallmarks for TGF-β signaling, MYC targets, and oxidative phosphorylation (Supplementary Fig. 9). (K) Differentially expressed genes were identified for T1-LumGU; overexpressed genes are shown by red dots and underexpressed by blue dots (Supplementary Fig. 10). This subtype had gene signatures suggestive of regulation by E2F and EZH2. Treatment of bladder cancer cell line HT-1376 with EPZ0011989 (Epizyme, Cambridge, MA, USA) resulted in increased expression of many of the repressed genes, depicted by orange dots, suggesting that subtype-specific genes may be regulated by EZH2. FC = fold change. The *p* values in A are from Fisher exact tests on contingency tables; those in E, F, and G are from Kruskal-Wallis tests on per-subtype FPKM distributions; all are uncorrected for multiple testing.

Table 1 – Characteristics of the five expression subtypes in the discovery cohort.

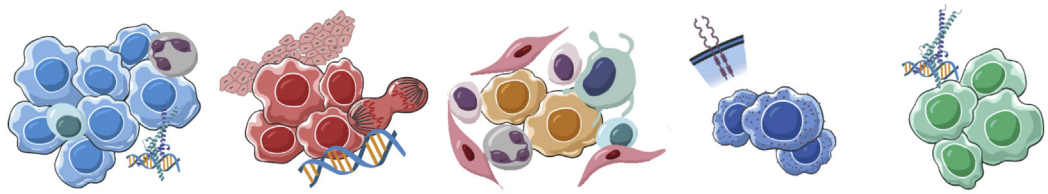

Subtype name (number)	T1-Myc (3)	T1-LumGU (1)	T1-Inflam (2)	T1-TLum (4)	T1-Early (5)
Samples (n)	17	16	14	13	13
Subtype classifiers					
Lund	URO	GU	URO, some Basal/ SCC-like, Mes-like	URO	URO
TCGA mRNA	Lum-papillary	Lum-papillary	Lum-papillary	Lum-papillary	Lum-papillary
consensusMIBC	LumP	LumU	LumP/Stroma-rich	LumP	LumP
UROMOL class	2a	2a	2a/2b	1/2a	2a/3
Hallmark gene sets					
Enriched		E2F targets, G2M checkpoint	Inflammatory response, IL2/STAT5 signaling, IFNG response		MYC targets v1
Repressed			MYC targets v1, E2F targets, G2M checkpoint	E2F targets G2M checkpoint	IFNG response IFNA response
Carcinoma in situ					
Pathologic (%)	12	38	21	15	0
GSEA		Moderate	Moderate	Strongly repressed	Weakly repressed
GSEA inflammation			Strongly enriched	Strongly repressed	Strongly repressed
Immune: MCPcounter					
CTLs			Highest	Lowest	Low
T cells			Highest median	Lowest	Lowest median
B lineage				Lowest median	Low
Immune: ESTIMATE					
Immune score	Low, wide range	Moderate, wide range	Highest	Low	Lowest median
Stromal score	Low	Low	Highest	Lowest median	Low
Tumor purity	High	High	Lowest	High	High
Gene expression	High FOXM1, RXRA Wide range for MYC	High E2F1, EZH2 Lowest FGFR3, MYC	High STAT4, NFATC2	Low E2F1, FOXM1, NFATC2, STAT4	High MYC, Low STAT4
CN somatic gains		Highest	Low	Lowest	Low
Activated regulons	Moderate E2F1	E2F1 set	TP63/ZNF385A	ZNF385A (TP63)	Moderate ZNF385A
BCG response					
Recurrence, 6 mo	3/17 (18%)	3/16 (19%)	1/14 (7%)	1/13 (8%)	5/13 (38%)
Recurrence, 24 mo	12/17 (53%)	4/16 (25%)	4/14 (29%)	2/13 (15%)	5/13 (38%)
Management	Early cystectomy, MYC-i	BCG, EZH2i	BCG	TURBT, BCG	Nadofaragene firadenovec, MYC-i

BCG = bacillus Calmette-Guerin; CN = copy number; CTLs = cytotoxic T lymphocytes; GSEA = gene set enrichment analysis; TURBT = transurethral resection of bladder tumor

SMAD3 and TP63 regulons, and enriched hallmarks for TGF-β signaling, MYC targets, and oxidative phosphorylation (Fig. 1J and Supplementary Fig. 7B). We found that these two major patterns of regulon activity were also present in a cohort of 94 UROMOL T1 non-cystectomy tumors; these patterns were consistent with classifier subtyping and with relative expression levels of E2F1 and other genes [7] (Supplementary Fig. 8). That the five expression subtypes corresponded to two major regulon activity classes suggests that regulon activity profiles may provide coarser-grained groupings for T1 tumors.

So that we could evaluate our subtypes in other patient cohorts, we developed an expression-based single-sample classifier for T1 tumors (https://github.com/csgroen/classifyT1BC). Since our discovery cohort was restricted to tumors treated with BCG, we evaluated tumors from a second cohort of 26 T1 patients from our institution whose tumors had all been T1 on TUR but who elected to undergo early cystectomy rather than BCG treatment (Supplementary Table 1B, Supplementary Fig. 9). The classifier identified the five T1 subtypes in the 26 tumors. As validation of the classifier, we identified conserved regulon activity patterns, relative levels of gene expression, tumor subtypes, and pathologic CIS in the predicted subtypes (Supplementary Fig. 9E). This result was consistent with the UROMOL results (Supplementary Fig. 8) and showed that gene expression and regulons active within our five T1 subtypes were conserved in another cohort of T1 tumors, despite differences in outcomes, sample preparation, and treatment.

One potential application of T1 subtypes is to direct precision therapy targeting the unique features of a patient's subtype. T1-LumGU tumors had the highest expression of E2F and its target EZH2. In a test of EZH2

as a potential target in bladder cancer, we found that in vitro treatment of the luminal bladder cancer cell line HT-1376 with an EZH2 inhibitor (EPZ-011989, a generous gift from Epizyme) strongly enhanced expression of DEGs that were repressed or underexpressed in T1-LumGU (Supplementary Fig. 10 and Fig. 1K). While preliminary, these data suggest that consideration of the unique expression signature of each subtype and/or its regulon network may identify novel therapeutic targets for T1 tumors.

In summary, using a cohort of patients with T1 NMIBC treated with BCG, we identified five distinct molecular subtypes that appeared to be associated with two major classes of regulon activity, and we describe the characteristics of each subtype. In the future, evaluation of T1 subtypes may help to risk-stratify T1 tumors and identify precision therapeutic targets.

Author contributions: Joshua J. Meeks had full access to all the data in the study and takes responsibility for the integrity of the data and the accuracy of the data analysis.
Study concept and design: Robertson, Meeks, Jordan, Lin, McLaughlin, Das, Fall, Taxter, Dyrskjøt, McConkey, Svatek, Castro, Fantini, Groeneveld, de Reyniès.
Acquisition of data: Robertson, Meeks, Jordan, Lin, McLaughlin, Das, Fall, Taxter, Dyrskjøt, McConkey, Svatek, Castro, Mogil, Viborg Lindskrog, Fantini.
Analysis and interpretation of data: Robertson, Meeks, Jordan, Lin, McLaughlin, Das, Fall, Taxter, Dyrskjøt, McConkey, Svatek, Castro, Mogil, Viborg Lindskrog, Fantini, Mogil, Groeneveld, de Reyniès.
Drafting of the manuscript: Robertson, Meeks, Jordan, Lin, McLaughlin, Das, Fall, Taxter, Dyrskjøt, McConkey, Svatek, Castro, Mogil, Viborg Lindskrog, Fantini, Mogil, Groeneveld, de Reyniès.
Critical revision of the manuscript for important intellectual content: Robertson, Meeks, Jordan, Lin, McLaughlin, Das, Fall, Taxter, Dyrskjøt, McConkey, Svatek, Castro, Mogil, Viborg Lindskrog, Fantini, Mogil, Groeneveld, de Reyniès.
Statistical analysis: Robertson, Meeks, Jordan, McLaughlin, Das, Taxter, Castro, Mogil, Viborg Lindskrog, Fantini, Groeneveld, de Reyniès.
Obtaining funding: Meeks, Svatek, McConkey.
Administrative, technical, or material support: None.
Supervision: Meeks, Svatek, Robertson, Dyrskjøt, Robertson, de Reyniès.
Other: None.

Financial disclosures: Joshua J. Meeks certifies that all conflicts of interest, including specific financial interests and relationships and affiliations relevant to the subject matter or materials discussed in the manuscript (eg, employment/affiliation, grants or funding, consultancies, honoraria, stock ownership or options, expert testimony, royalties, or patents filed, received, or pending), are the following: Joshua J. Meeks is a consultant for Ferring, AstraZeneca, and Janssen and has participated in advisory boards for Foundation Medicine and Nucleix. The remaining authors have nothing to disclose.

Funding/Support and role of the sponsor: Joshua J. Meeks is supported by grants from VHA (BX003692-01), DoD (W81XWH-18-0257), the Dixon Foundation, and a HOPE Foundation SEED award. The sponsors played a role in the design and conduct of the study.

Acknowledgments: We gratefully acknowledge Mao Miyamoto for contributing the illustrations for Table 1, and Epizyme (Cambridge MA) for contributing the EZH2 inhibitor EPZ-011989.

Data availability: RNA-seq and clinical data are available at the Gene Expression Omnibus as GSE154261.

Appendix A. Supplementary data

Supplementary material related to this article can be found, in the online version, at doi:https://doi.org/10.1016/j.eururo.2020.06.048.

References

[1] van den Bosch S, Witjes JA. Long-term cancer-specific survival in patients with high-risk, non-muscle-invasive bladder cancer and tumour progression: a systematic review. Eur Urol 2011;60:493–500.
[2] Meeks JJ, Carneiro BA, Pai SG, et al. Genomic characterization of high-risk non-muscle invasive bladder cancer. Oncotarget 2016;7:75176–84.
[3] Pennock ND, Jindal S, Horton W, et al. RNA-seq from archival FFPE breast cancer samples: molecular pathway fidelity and novel discovery. BMC Med Genomics 2019;12:195.
[4] Kamoun A, de Reyniès A, Allory Y, et al. A consensus molecular classification of muscle-invasive bladder cancer. Eur Urol 2020;77:420–33.
[5] Zyla J, Marczyk M, Domaszewska T, Kaufmann SHE, Polanska J, Weiner J. Gene set enrichment for reproducible science: comparison of CERNO and eight other algorithms. Bioinformatics 2019;35:5146–54.
[6] Beaubier N, Bontrager M, Huether R, et al. Integrated genomic profiling expands clinical options for patients with cancer. Nat Biotechnol 2019;37:1351–60.
[7] Hedegaard J, Lamy P, Nordentoft I, et al. Comprehensive transcriptional analysis of early-stage urothelial carcinoma. Cancer Cell 2016;30:27–42.